Check for updates

The Photorespiratory Metabolite 2-Phosphoglycolate Regulates Photosynthesis and Starch Accumulation in Arabidopsis

Franziska Flügel,[a] Stefan Timm,[a] Stéphanie Arrivault,[b] Alexandra Florian,[b] Mark Stitt,[b] Alisdair R. Fernie,[b] and Hermann Bauwe[a,1]

[a] Plant Physiology Department, University of Rostock, D-18051 Rostock, Germany
[b] Max Planck Institute of Molecular Plant Physiology, D-14476 Potsdam-Golm, Germany

ORCID IDs: 0000-0003-3105-6296 (S.T.); 0000-0002-4900-1763 (M.S.); 0000-0001-7802-8925 (H.B.)

The Calvin-Benson cycle and its photorespiratory repair shunt are in charge of nearly all biological CO_2 fixation on Earth. They interact functionally and via shared carbon flow on several levels including common metabolites, transcriptional regulation, and response to environmental changes. 2-Phosphoglycolate (2PG) is one of the shared metabolites and produced in large amounts by oxidative damage of the CO_2 acceptor molecule ribulose 1,5-bisphosphate. It was anticipated early on, although never proven, that 2PG could also be a regulatory metabolite that modulates central carbon metabolism by inhibition of triose-phosphate isomerase. Here, we examined this hypothesis using transgenic _Arabidopsis thaliana_ lines with varying activities of the 2PG-degrading enzyme, 2PG phosphatase, and analyzing the impact of this intervention on operation of the Calvin-Benson cycle and other central pathways, leaf carbohydrate metabolism, photosynthetic gas exchange, and growth. Our results demonstrate that 2PG feeds back on the Calvin-Benson cycle. It also alters the allocation of photosynthates between ribulose 1,5-bisphosphate regeneration and starch synthesis. 2PG mechanistically achieves this by inhibiting the Calvin-Benson cycle enzymes triose-phosphate isomerase and sedoheptulose 1,7-bisphosphate phosphatase. We suggest this may represent one of the control loops that sense the ratio of photorespiratory to photosynthetic carbon flux and in turn adjusts stomatal conductance, photosynthetic CO_2 and photorespiratory O_2 fixation, and starch synthesis in response to changes in the environment.

INTRODUCTION

2-Phosphoglycolate (2PG) is an important metabolite in many organisms. In mammals, it activates the 2,3-bisphosphoglycerate phosphatase module of the erythrocyte-specific trifunctional enzyme bisphosphoglycerate mutase: Binding of 2PG stimulates the phosphatase activity of this protein up to 1600-fold, lowering the content of 2,3-bisphosphoglycerate, which dissociates from and increases the affinity to O_2 of hemoglobin (Rose and Liebowitz, 1970; Sasaki et al., 1975). The exact origin of 2PG in heterotrophic organisms remains unknown (Sasaki et al., 1987; Knight et al., 2012). A small quantity is produced during processing of the 3'-PG terminated DNA strand breaks (Winters et al., 1994), but there may be additional sources of 2PG in these organisms.

Plants and other oxygenic autotrophs produce 2PG mostly in an O_2-dependent side reaction of the CO_2 fixation enzyme ribulose 1,5-bisphosphate (RuBP) carboxylase (Rubisco; Bowes et al., 1971). The resulting RuBP damage (Linster et al., 2013) is repaired in the multistep photorespiratory pathway via the conversion of 2PG to 3-phosphoglycerate (3PGA), the actual product of RuBP carboxylation, from which RuBP is eventually regenerated in the Calvin-Benson cycle (CBC). The conversion process releases one molecule of "photorespiratory" CO_2 per every two recycled 2PG

molecules, thereby reducing net photosynthesis. This is why over the last decades, photorespiration has been seen as an attractive target for the breeding of high-yield crops (Zelitch, 1975; Ort et al., 2015; Betti et al., 2016).

Efficient recycling of 2PG is particularly important in C_3 plants, which produce 2PG in large amounts. If 2PG were to accumulate, this would sequester correspondingly large amounts of C and P, resulting in draining of the CBC's metabolite pool (Wingler et al., 2000). Additionally, 2PG is a potentially toxic metabolite (Hall et al., 1987) because it inhibits at least two key enzymes of chloroplast carbon metabolism, namely, triose-phosphate isomerase (TPI), which is needed both in the CBC and for starch synthesis ($K_i \sim 15\,\mu M$ in pea [_Pisum sativum_] leaves; Anderson, 1971), and phosphofructokinase, which is a glycolytic enzyme downstream of starch degradation ($K_i \sim 50\,\mu M$ in spinach [_Spinacia oleracea_] leaves; Kelly and Latzko, 1976). Temporarily altered fluxes through the photorespiratory pathway such as those that often occur during the day could alter the levels of photorespiratory intermediates including 2PG, and this might influence CBC activity and other photosynthesis-related processes. This hypothesis also explains the changes in photosynthesis and growth observed as a result of an artificially altered activity of the glycine cleavage system, which catalyzes another crucial step in the photorespiratory pathway (Heineke et al., 2001; Timm et al., 2012a, 2015).

The breakdown of 2PG is catalyzed by homologs of the ubiquitous enzyme 2PG phosphatase (PGLP; EC 3.1.3.18), which are metabolite damage repair enzymes with multiple functions. In oxygenic autotrophs, they catalyze the first step of the photorespiratory pathway, and in mammals, yeast, and possibly other organisms, they remove

---

2PG and destroy toxic side products of glycolysis (Beaudoin and Hanson, 2016; Collard et al., 2016). The human erythrocyte PGLP is redox controlled (Seifried et al., 2016) and additionally acts as a glycerol 3-phosphate phosphatase, regulating a number of metabolic processes including glycolysis and gluconeogenesis and the response to metabolic stress (Mugabo et al., 2016). The enzyme typically is an ~66-kD homodimer. Similarities of the kinetic and other properties of PGLPs from different organisms point to a common evolutionary starting point (Rose et al., 1986), possibly in the Archaean-like ancestor of the eukaryotic cell (Hagemann et al., 2016).

Arabidopsis thaliana harbors two PGLP isoenzymes, one located in the plastid (PGLP1, At5g36700) and one in the cytosol (PGLP2, At5g47760), with each being encoded by a single gene. Loss-of-function mutants of the cytosolic isoform are not obviously different from the wild type, whereas elimination of PGLP1 results in a conditionally lethal phenotype: lethal in normal air but largely vital in a high-CO_2 environment, which inhibits the oxygenation of RuBP and favors carboxylation (Somerville and Ogren, 1979; Schwarte and Bauwe, 2007). A PGLP-deficient mutant of barley (*Hordeum vulgare*) shows features that are very similar to the Arabidopsis *PGLP1* mutant (Hall et al., 1987). Historically, these mutagenesis experiments resolved the prolonged dispute of whether the glycolate used in the photorespiratory pathway originates from RuBP oxygenation or rather from other cellular processes.

Previous investigations on the impact of PGLP1 deficiency on plant metabolism focused on loss-of-function mutants (Timm et al., 2012b; Eisenhut et al., 2017). However, metabolic regulation can be more usefully studied in genotypes with smaller changes in expression (Stitt et al., 2010), especially for genes whose deletion shows such major effects on metabolism and growth as *PGLP1*. In this study, we examined Arabidopsis plants with more moderately modified leaf PGLP1 activity, above and below wild-type level, using the wild type and a *PGLP1* knockout mutant as controls, with the aim to find out to what extent such changes would alter leaf 2PG levels and in turn photosynthesis and other central carbon metabolism.

RESULTS

Fine Adjustment of PGLP Activity by Antisense Suppression and Overexpression

As mentioned before, *PGLP1* knockout mutants require very high levels of CO_2 (1%, high CO_2 [HC]) for growth and do not survive in normal air (presently 0.04%, low CO_2 [LC]), in which they display an increasing number of pleiotropic alterations before they eventually die. For that reason, building on the identification of the Arabidopsis *PGLP1* gene (Schwarte and Bauwe, 2007), we produced three sets of transgenic plants. First, as a routine precaution, we retransformed the Arabidopsis *PGLP1* loss-of-function mutant (*pglp1*) with a complementation construct comprising the Arabidopsis *PGLP1* coding sequence (CDS) under control of the cauliflower mosaic virus (CaMV) 35S promoter (Supplemental Figure 1A). Three independently transformed lines expressing the transgenic *PGLP1* were selected for growth in normal air

(Supplemental Figure 2). They were indistinguishable from the wild type by visual inspection and displayed wild-type-like values for the net rate of CO_2 uptake (A), the CO_2 compensation point at 21% O_2 (Γ_{21}), and starch content. This reconfirmed that the *pglp1* locus and not a hidden background mutation is responsible for the metabolic features and growth responses of this mutant. Second, we produced a series of transgenic Arabidopsis plants with a gradual decrease in PGLP1 activity by expressing the *PGLP1* cDNA in antisense orientation under control of the CaMV 35S promoter (Supplemental Figure 1B). Third, in order to study the effect of higher PGLP1 activity, we overexpressed *PGLP1* under control of the strong light-inducible *Solanum tuberosum leaf/stem specific 1* (*ST-LS1*) gene promoter (Stockhaus et al., 1989; Supplemental Figure 1C).

RT-qPCR demonstrated that expression of *PGLP1* showed a range of transcript levels, from zero in *pglp1* via 9% (A1), 18% (A8), and 68% (A2) of wild-type level in three antisense lines and 140% (O8), 180% (O1), and 203% (O9) in three overexpression lines (Figure 1A). Altered gene expression translated into altered leaf PGLP1 protein content, as determined by immunoblotting using a specific antibody raised against recombinant Arabidopsis PGLP1 (Figure 1B). We propagated all these lines to yield stable T4 progenies and measured leaf PGLP enzyme activities. Corresponding to the changes observed on the transcript level, the result shows that total PGLP activity progressively decreased (down to ~9% in line A1) or increased (up to ~144% in line O1) compared with the wild type (Figure 1C). The correlation between PGLP activity and transcript contents is highly significant (Spearman rank correlation coefficient $\rho = 0.976$**; Supplemental Table 1).

Gradually Changed PGLP1 Activity Alters Growth and Photosynthesis

All antisense lines grew well under HC conditions. In LC conditions, line A2 also grew well though with a slight growth reduction (Figure 1D) and produced fertile seeds, while line A8 and particularly line A1, in which only little PGLP1 activity is left, were more severely impaired. They grew slowly, had a pale-green appearance, flowered somewhat later, and did not form viable seeds in normal air. Given the slower growth of all antisense lines including A2, the one with the smallest reduction in leaf PGLP activity, we next examined whether more PGLP1 activity would improve growth. To this end, we grew the three overexpressor lines and the wild type in LC to growth stage 5.1 according to Boyes et al. (2001), which is reached after 8 weeks, and measured several quantitative growth parameters. The results in Table 1 demonstrate that higher PGLP1 activity indeed slightly improved growth, as seen by the up to 13% larger rosette diameter (significant in all three lines), ~11% more leaves, and 5 to 9% and 6% higher fresh and dry weight, respectively. These increases were significant in O9 and O1.

Growth is ultimately dependent on photosynthetic CO_2 fixation. To examine the effects of lower PGLP1 activity on photosynthesis, we grew *pglp1* and the antisense lines side by side with wild-type plants under HC conditions for 8 weeks followed by transfer to LC conditions. This growth protocol was dictated by the air sensitivity of several of the examined genotypes and used to ensure the greatest possible comparability between the genotypes. The day
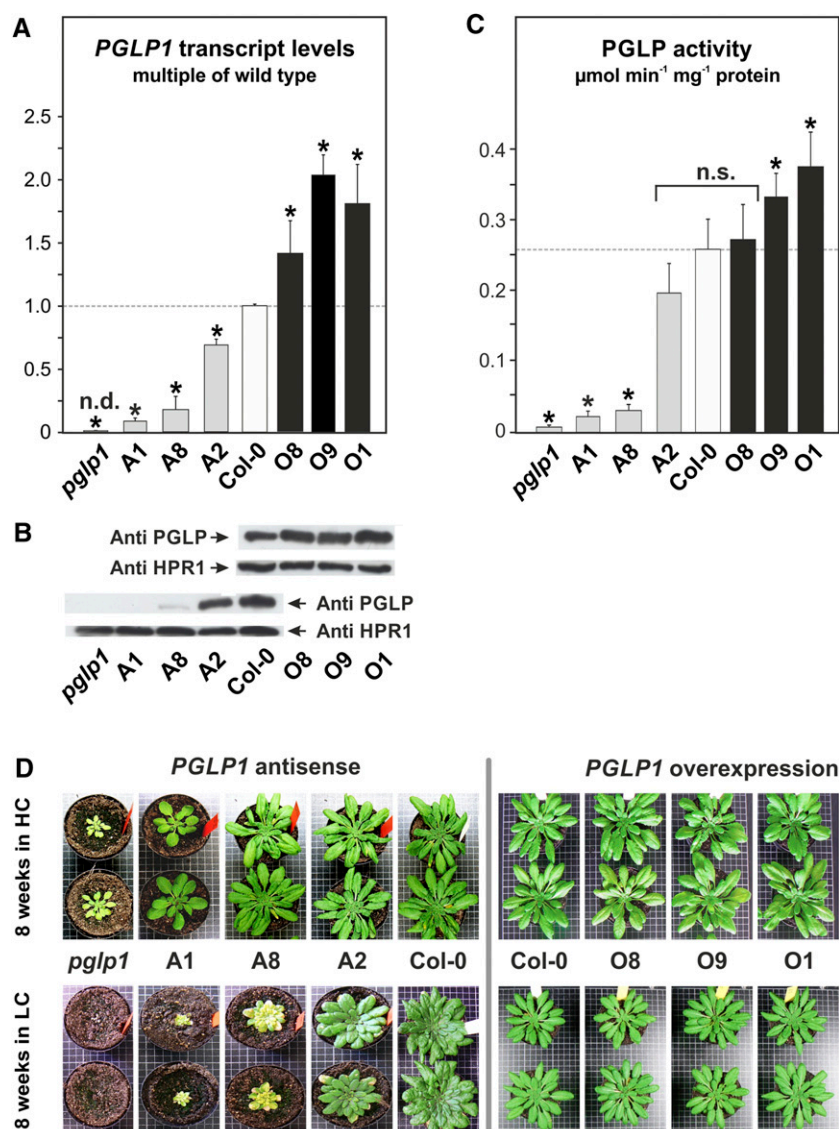
Figure 1. *PGLP1* Expression, Leaf PGLP Enzymatic Activity, and Plant Growth.

(A) RT-qPCR quantification of *PGLP1* expression in leaves of transgenic lines. The wild-type signal was arbitrarily set to 1.

(B) Immunoblot of leaf proteins using a specific antibody against PGLP1 and Hydroxypyruvate Reductase 1 (HPR1) as control.

(C) PGLP enzymatic activity in leaves.

(D) Antisense and overexpressor plants after growth for 8 weeks, 10-h photoperiod, in air enriched with 1% CO_2 (HC) or normal air (LC).

Values in **(A)** and **(C)** are means $\pm$ SD (five different plants per genotype). Asterisks indicate values significantly different from the wild type based on Student's *t* test (*P < 0.05; n.d., not detectable; n.s., not significant).

before and at days 1, 3, 5, and 7 after transfer from HC to LC, maximum quantum yield of PSII (F_v/F_m), net CO_2 uptake rates, and CO_2 compensation points at 21% O_2 were determined (Figure 2). F_v/F_m values were not clearly different between the lines in HC except for significantly lower values for *pglp1*. Following transfer to normal air, F_v/F_m progressively decreased in lines with decreased PGLP activity (A2 > A8 > A1 > *pglp1*), proportionally to the PGLP activity gradient, but did not significantly change in the wild type. F_v/F_m was unaltered in the *PGLP1* overexpression lines in

comparison with the wild type both in HC and in LC conditions (data not shown). Corresponding to these variations in the linear photosynthetic electron transport efficiency, values for A decreased and values for Γ_{21} increased in response to lower PGLP1 activity. We also observed significantly lower stomatal conductances (g_s) and transpiration rates (E) in the antisense lines following short-term adaptation to LC (Table 2).

Given that the above data indicate that Arabidopsis responds sensitively to even a slight reduction in PGLP activity, we next

Table 1. Growth of *PGLP1* Overexpressors and the Wild Type

Parameter	Col-0	O8	O9	O1
Diameter (cm)	9.1 ± 0.55	**9.6 ± 0.61**	**9.8 ± 0.40**	**10.3 ± 0.41**
Leaf number	25.7 ± 1.65	26.4 ± 2.06	**27.8 ± 1.42**	**28.6 ± 2.54**
Fresh weight (g)	4.3 ± 0.17	4.3 ± 0.11	**4.5 ± 0.24**	**4.7 ± 0.22**
Dry weight (g)	0.55 ± 0.02	0.56 ± 0.03	**0.58 ± 0.04**	**0.59 ± 0.02**

Plants were grown in a 10-h photoperiod, 20/18°C day/night, in LC to growth stage 5.1 (Boyes et al., 2001). Values are means ± SD for rosette leaves (20 different plants per genotype). Numbers in bold are significantly higher than the wild-type value based on Student's *t* test (P < 0.05).

examined how the photosynthetic performance of the over-expressor plants would react to lower and higher photo-respiratory pressure. As shown in Table 2, all overexpressor lines display between 50 and 70% higher stomatal con-ductances at 40% O_2, which extends the trend observed with the antisense lines. Net CO_2 fixation is almost unaltered at 10% and 21% O_2, but in all three lines was significantly faster than in the wild type at 40% O_2, a concentration that considerably boosts 2PG generation. Values for Γ at 40% O_2 and the O_2 inhibition of CO_2 fixation at 40% versus 21% O_2 were signifi-cantly lower than in the wild type only in line O1, which exhibits the highest PGLP1 activity. This line also showed slightly but significantly higher rates of photorespiration (R_p), corresponding to the faster CO_2 uptake, and higher nighttime respiration (R_n).

PGLP1 Activity Modulates 2PG Levels and Operation of the Calvin-Benson Cycle

We next examined to what extent altered PGLP1 activity affects the levels of metabolites, with an emphasis on metabolites in photorespiration, the CBC, and starch and sucrose biosynthesis. To this end, two sets of leaf samples from HC-grown plants, before and after exposure to LC for 5 h, were harvested after 5 h illumination (middle of the day [MoD]). It should be noted that metabolite de-termination by gas chromatography-mass spectrometry (GC-MS) was performed in a qualitative manner in all lines, while metabolite determination by liquid chromatography-tandem mass spec-trometry (LC-MS/MS) was performed in a quantitative manner in the lines with distinctly altered PGLP activity (*pglp1*, A1, A8, wild type, O9, and O1), omitting the genotypes (A2 and O8) that were most similar to the wild type. The results for the phosphorylated metabolites in HC and LC conditions are shown in Figure 3 (LC-MS/MS data) and as heat maps of the nonphosphorylated metabolites in Figure 4 (GC-MS data). For the numerical values, see Supplemental Data Sets 1 and 2. Spearman correlation coefficients ρ were calculated in order to see whether the changes in metabolite contents correlate with the altered PGLP activity (Supplemental Table 1).

Under the low-photorespiratory HC condition, the wild type had a very low level of 2PG (0.4 nmol g^{-1} FW). Even in this condition where photorespiration will be slow, *pglp1* (240 nmol g^{-1} FW) and antisense line A1 (11 nmol g^{-1} FW) exhibited massively increased 2PG contents, and there was a significant increase in line A8 (0.8 nmol g^{-1} FW). There was no change in the two examined overexpressor lines, O9 and O1.

Under the high-photorespiratory LC condition, the 2PG content increased to the very high levels of 1100, 720, and 470 nmol g^{-1}

FW in *pglp1* and lines A1 and A8, respectively, and to some extent in the wild type (1.8 nmol g^{-1} FW), compared with the wild-type level in HC. The two overexpressor lines with higher PGLP1 ac-tivities displayed slightly but significantly lower 2PG contents (0.7 nmol g^{-1} FW in O9 and 1.1 nmol g^{-1} FW in O1) than wild-type plants. Taken all genotypes together, the 2PG contents are significantly correlated with PGLP activity (ρ = −0.943**) in LC but not in HC. Additionally, the data in Figure 4 show that gly-colate accumulates in some lines with very low PGLP activity in HC (*pglp1*) and LC (*pglp1* and A1). This effect is known from recent work with *pglp1* (Eisenhut et al., 2017) though the path leading to glycolate accumulation under extreme PGLP1 de-ficiency is unknown. Apart from 2PG, glycine was the only other metabolite of the photorespiratory pathway that displayed signifi-cant changes with higher (*pglp1* and A1) and lower (overexpression lines O9 and O1) levels compared with the wild type in LC (correlated with PGLP activity over all genotypes, ρ = −0.952**). These changes were also apparent in HC (Supplemental Figure 3; ρ = −0.786*).

Among the CBC intermediates under HC conditions, the dominant effect was found in the contents of sedoheptulose 7-phosphate (S7P), which were lower in both antisense lines (A1 < A8 < Col-0) and although to a lesser extent also in the overexpressor lines (Col-0 > O9 > O1). A similar but less pro-nounced tendency of higher contents in the wild type than in the antisense and overexpressor lines was observed for 3PGA and NADP. This pattern was not consistently seen for other CBC metabolites such as RuBP, dihydroxyacetone phosphate (DHAP), sedoheptulose 1,7-bisphosphate (SBP), ribose 5-phosphate (R5P), and ribulose 5-phosphate together with xylulose 5-phosphate (Ru5P+X5P). Intermediates of starch and/or sucrose synthesis including fructose 1,6-bisphosphate (FBP), glucose 6-phosphate (G6P), glucose 1-phosphate (G1P), adenosine 5′-diphosphate glucose (ADPG; Figure 5A), and uridine 5′-diphosphate glucose (UDPG) did not show any consistent genotype-dependent changes in HC, except for a decrease in fructose 6-phosphate (F6P) in *pglp1* and A1.

In LC, the contents of most of the analyzed CBC intermediates (RuBP, 3PGA, DHAP, FBP, F6P, SBP, S7P, and R5P) fell to much lower levels in *pglp1* and at least one of the two antisense lines compared with wild-type plants. RuBP, 3PGA, DHAP, and S7P also decreased, but to a lesser extent, in the overexpressors. The changes in SBP (ρ = 0.829*) and S7P (ρ = 0.829*) in LC are positively correlated with alterations in PGLP activity. As ex-pected, the changes in these two metabolites appear to be negatively correlated with alterations in the 2PG content, but neither of these correlations is statistically significant (ρ = −0.771 and P = 0.103 for both SBP and S7P). Intermediates of starch and

Figure 2. Maximum Quantum Efficiency of PSII and Gas Exchange.

(A) Chlorophyll *a* fluorescence images and F_v/F_m color codes.
(B) PSII quantum efficiency F_v/F_m.

sucrose synthesis decreased in *pglp1* and the antisense lines (G6P in A1; G1P in A8) but were not clearly altered in the *PGLP1* overexpressors. NADP (*pglp1* and line A1) and ADP (lines A1, A8, O9, and O1) show lower levels in LC but, as in HC, without an accompanying corresponding change in NAD and AMP. Notably, the content of ADPG fell much more in the antisense lines and *pglp1* than the content of UDPG (Figure 5A).

This analysis on the whole-leaf level cannot differentiate between plastidic (CBC and starch synthesis) and cytosolic (sucrose synthesis) metabolites, except for RuBP, SBP, and ADPG, which are localized exclusively in the plastid, and UDPG, which is largely confined to the cytosol (Szecowka et al., 2013). Nevertheless, our data clearly demonstrate that an altered 2PG content changes metabolite levels in the CBC, both on the antisense and the overexpression side. The general decline in metabolite levels in low-PGPL1 lines in LC may reflect the sequestration of C and P in the large pool of 2PG. However, particularly for F6P and S7P, such changes were visible already under HC conditions, suggesting that 2PG could interact not only with TPI but also with SBPase and maybe further enzymes of the CBC.

In order to confirm that 2PG inhibits Arabidopsis TPI and to test the possibility that it may additionally inhibit SBPase, we measured the effect of 2PG on Arabidopsis TPI activity and performed initial studies on SBPase. For TPI, we found a clear competitive inhibition by 2PG with an approximate K_i of 36 ± 4 μM (Supplemental Figure 4), which is close to the K_i of 15 μM 2PG reported for pea TPI (Anderson, 1971). SBPase could not be measured in a classical assay (Dunford et al., 1998) because in the presence of 2PG an unidentified component of the assay interfered with phosphate determination. Instead, we designed an LC-MS/MS-based approach for the determination of S7P release rates. Using this new assay, we found that 2PG indeed is an effective inhibitor of SBPase (Supplemental Figure 5A). The measured decrease in enzyme activity by ~65% in the presence of 130 μM 2PG would correspond to a K_i around 10 μM 2PG (Supplemental Figure 5C). This rough calculation was performed using the standard kinetic equation for competitive enzyme inhibition with a K_m for SBP of 13 μM (Marques et al., 1987) and the concentrations of SBP and 2PG in the assay, which were 130 μM each. It must be noted that some initial activation of the enzyme occurs and that S7P production slows down after 5 to 6 min. These two effects are likely due to activation of the enzyme by the SBP substrate and later to end-product inhibition by S7P (Schimkat et al., 1990).

(C) Net photosynthetic CO_2 uptake.
(D) CO_2 compensation points Γ_{21}.
Plants were grown for 8 weeks in HC as described in Figure 1D and then transferred to LC. PSII fluorescence and gas exchange parameters were determined at days 0 (H) and 1, 3, 5, and 7 d after transfer to normal air. Data for the *pglp1* mutant are included for comparison from a previous study (Timm et al., 2012b). Bars represent means $\pm$ SD (five different plants per genotype). Asterisks indicate values significantly different from the HC control and plus signs from the respective wild-type value based on Student's *t* test (*P < 0.05).

Table 2. Gas Exchange of *PGLP1* Antisense and Overexpressor Lines

Parameter	*pglp1*	A1	A8	A2	Col-0
g_s HC	**0.08 ± 0.02**	**0.07 ± 0.02**	**0.20 ± 0.01**	0.12 ± 0.03	0.12 ± 0.01
g_s 1 d LC	**0.05 ± 0.01**	**0.06 ± 0.01**	**0.06 ± 0.01**	**0.07 ± 0.01**	0.12 ± 0.02
E HC	1.63 ± 0.40	**1.09 ± 0.22**	**2.56 ± 0.09**	1.65 ± 0.23	1.63 ± 0.13
E 1 d LC	**0.83 ± 0.18**	**1.08 ± 0.23**	**1.12 ± 0.20**	**1.34 ± 0.23**	1.87 ± 0.18
		O1	O9	O8	Col-0
g_{s10}		0.22 ± 0.07	0.22 ± 0.05	0.24 ± 0.03	0.18 ± 0.04
g_{s21}		0.30 ± 0.05	0.24 ± 0.03	0.27 ± 0.06	0.26 ± 0.04
g_{s40}		**0.23 ± 0.06**	**0.26 ± 0.03**	**0.23 ± 0.03**	0.15 ± 0.03
A_{10}		13.54 ± 1.14	13.74 ± 2.06	14.36 ± 0.66	13.56 ± 0.84
A_{21}		12.09 ± 1.87	12.26 ± 1.17	12.32 ± 1.45	11.35 ± 1.52
A_{40}		**8.33 ± 0.55**	**7.46 ± 0.68**	**8.10 ± 1.69**	6.20 ± 0.58
O_2 inhibition		**30.28 ± 7.31**	38.85 ± 6.49	43.27 ± 9.88	44.98 ± 5.26
Γ_{10}		26.0 ± 4.50	24.2 ± 4.92	21.8 ± 5.07	24.6 ± 3.68
Γ_{21}		57.9 ± 10.3	62.2 ± 9.04	55.9 ± 5.55	62.0 ± 3.54
Γ_{40}		**104.1 ± 4.48**	118.8 ± 8.57	114.4 ± 12.2	111.0 ± 3.29
$\Gamma_{21}{}^{*}$		36.6 ± 1.54	27.9 ± 4.66	28.1 ± 4.38	32.9 ± 3.93
R_n		**1.03 ± 0.10**	1.07 ± 0.20	1.08 ± 0.16	0.84 ± 0.12
R_d		1.21 ± 0.08	1.33 ± 0.18	1.27 ± 0.29	1.36 ± 0.24
R_p		**1.76 ± 0.24**	1.54 ± 0.37	1.45 ± 0.17	1.38 ± 0.08

Antisense and overexpressor plants were grown in HC and LC, respectively, under conditions as in Figure 1D. Stomatal conductance and transpiration of antisense plants were measured before and at day 1 after transfer from HC to LC. Values are means ± SD (at least four different plants per genotype). Numbers in bold are significantly different from the wild-type value based on Student's *t* test (P < 0.05). Units are mol H_2O m^{-2} s^{-1} (g_s), μmol CO_2 m^{-2} s^{-1} (A, R_d, R_n, and R_p), μL L^{-1} (Γ and $\Gamma_{21}{}^{*}$), and mmol H_2O m^{-2} s^{-1} (E). O_2 inhibition of A was calculated as 100(A_{21} − A_{40})/A_{21}. Values for the *pglp1* mutant are included for comparison from a previous study (Timm et al., 2012b). A, net CO_2 uptake; Γ, CO_2 compensation point; $\Gamma_{21}{}^{*}$, Γ_{21} corrected for day respiration; g_s, stomatal conductance; R_d, daytime respiration; R_n, nighttime respiration; R_p, photorespiration; indices are 10, 21, and 40% O_2.

Starch but Not Sucrose Biosynthesis Responds to Altered PGLP1 Activity

We reported earlier that *pglp1* accumulates very little starch during the day, which is not a typical feature of other photorespiratory mutants (Timm et al., 2012b). However, it corresponds well to the abovementioned lower content of ADPG in all three low-PGLP1 lines under LC. In order to examine the impact of gradually altered PGLP1 activity on starch synthesis, which would also show whether the low-starch feature of the knockout mutant is directly caused by PGLP1 deficiency and not by unknown secondary effects, we grew all genotypes in HC followed by adaptation to LC as described before. Leaf samples were harvested at the end of the day (EoD; 9 h illumination) in HC and 24 h later after 9 h in LC. As shown in Figure 5, leaf starch contents did not significantly differ under HC conditions, except for *pglp1*, in which it was ~30% lower. After exposure to LC, however, starch contents of all genotypes became significantly different from the wild-type control, being lower in all antisense plants and slightly but significantly higher in the overexpressor lines O9 and O1. By rank correlation, EoD starch content is positively correlated with PGLP1 activity in HC ($\rho = 0.952$**) and LC ($\rho = 0.999$**) and with net photosynthetic CO_2 uptake in HC ($\rho = 0.900$*) and LC ($\rho = 0.999$**). We also determined rates of starch accumulation and remobilization in LC-grown overexpression lines and the wild type from samples harvested in eight consecutive intervals over one day-night cycle (Figure 5C). The calculated rates suggested that starch synthesis is significantly faster in the two lines with the highest PGLP1 activity (O9 and O1), whereas starch degradation is slightly but significantly enhanced only in line O1. Note that

these changes were not accompanied by altered expression of the genes encoding phosphoglucomutase (PGM), phosphoglucoisomerase (PGI), and TPI in HC and LC (Supplemental Figure 6), indicating that they are largely caused by alleviation of the inhibition of TPI and SBPase by 2PG.

It was earlier suggested (Somerville and Ogren, 1979) that elevated 2PG could favor export of triose-phosphate out of the chloroplast for enhanced sucrose biosynthesis. In order to test this possibility, we also analyzed leaf sucrose levels at EoD in HC and LC using an enzymatic assay. With the exception of somewhat lower values for *pglp1* leaves in both conditions and in line A2 in HC, sucrose contents did not differ significantly between the eight analyzed genotypes in either LC or HC, which corresponds to the GC-MS sucrose data (Supplemental Data Set 2). This result also corresponds to the unaltered UDPG contents of all genotypes in HC (Figure 5A). The lower values for *pglp1* and the two examined antisense lines in LC may suggest that both the synthesis and the export of sucrose are reduced in these lines compared with the wild type. However, because sucrose contents depend on the rates of its synthesis and export, a substantiated conclusion will require flux studies. Collectively, these data show that starch biosynthesis but not the steady state leaf sucrose contents responds to altered PGLP1 activity and in turn altered 2PG levels.

Altered PGLP1 Activity Induces Changes in Organic Acid and Amino Acid Metabolism Including the GABA Shunt

For the nonphosphorylated metabolites outside the CBC, changes were less or not visible in most of the examined lines, both in HC
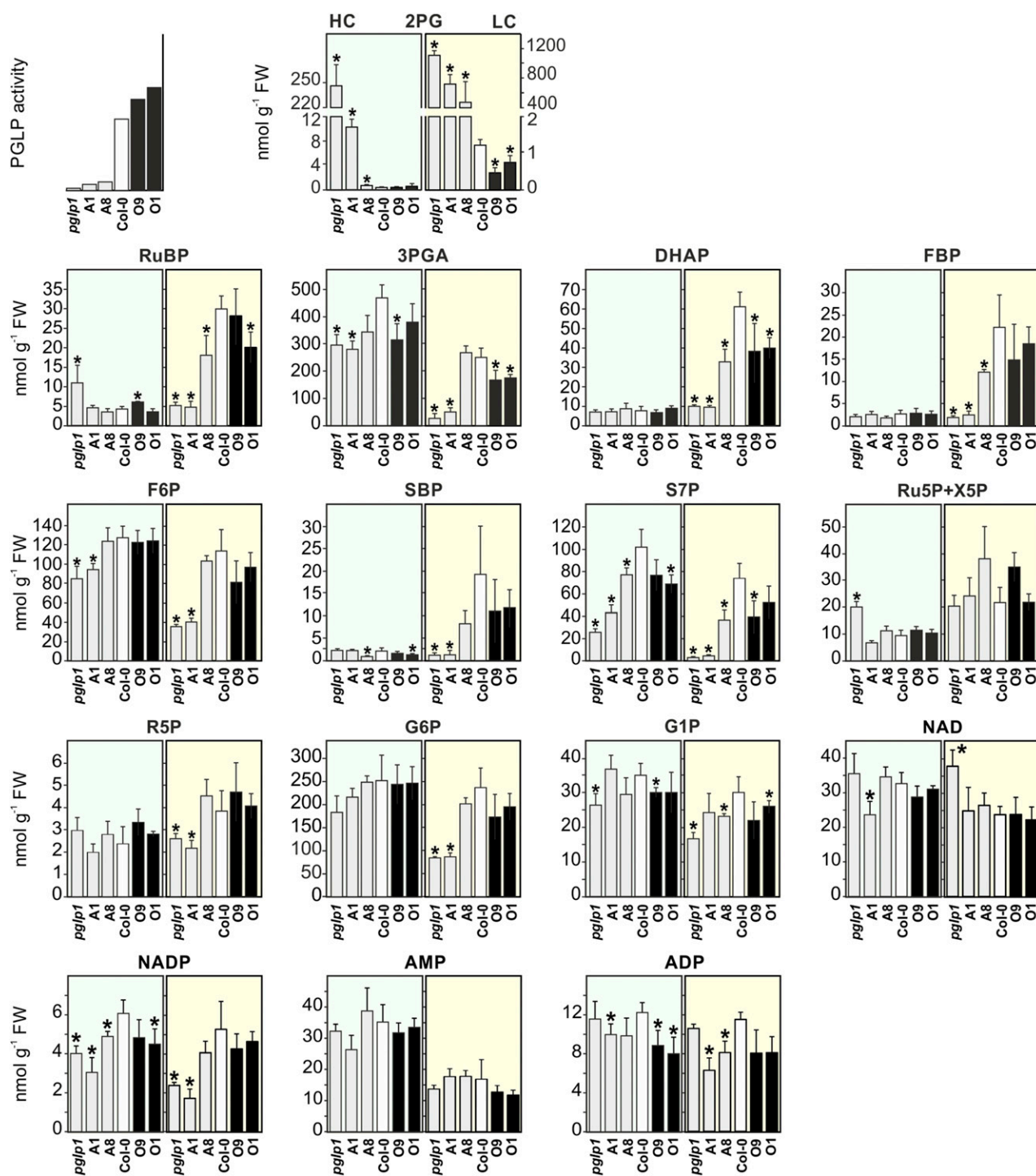
Figure 3. Intermediates of the Calvin-Benson Cycle, Photorespiration, and Sucrose and Starch Synthesis.

Leaf samples were harvested at MoD (5 h after first light) from plants grown in HC as described in Figure 1D and the next MoD after 5 h exposure to LC. Concentrations are in nmol g^{-1} fresh weight. Columns represent means ± SD (four different plants per genotype). Asterisks indicate values significantly different from the wild type based on Student's t test (*$P < 0.05$). See Supplemental Data Set 1 for the numerical data.
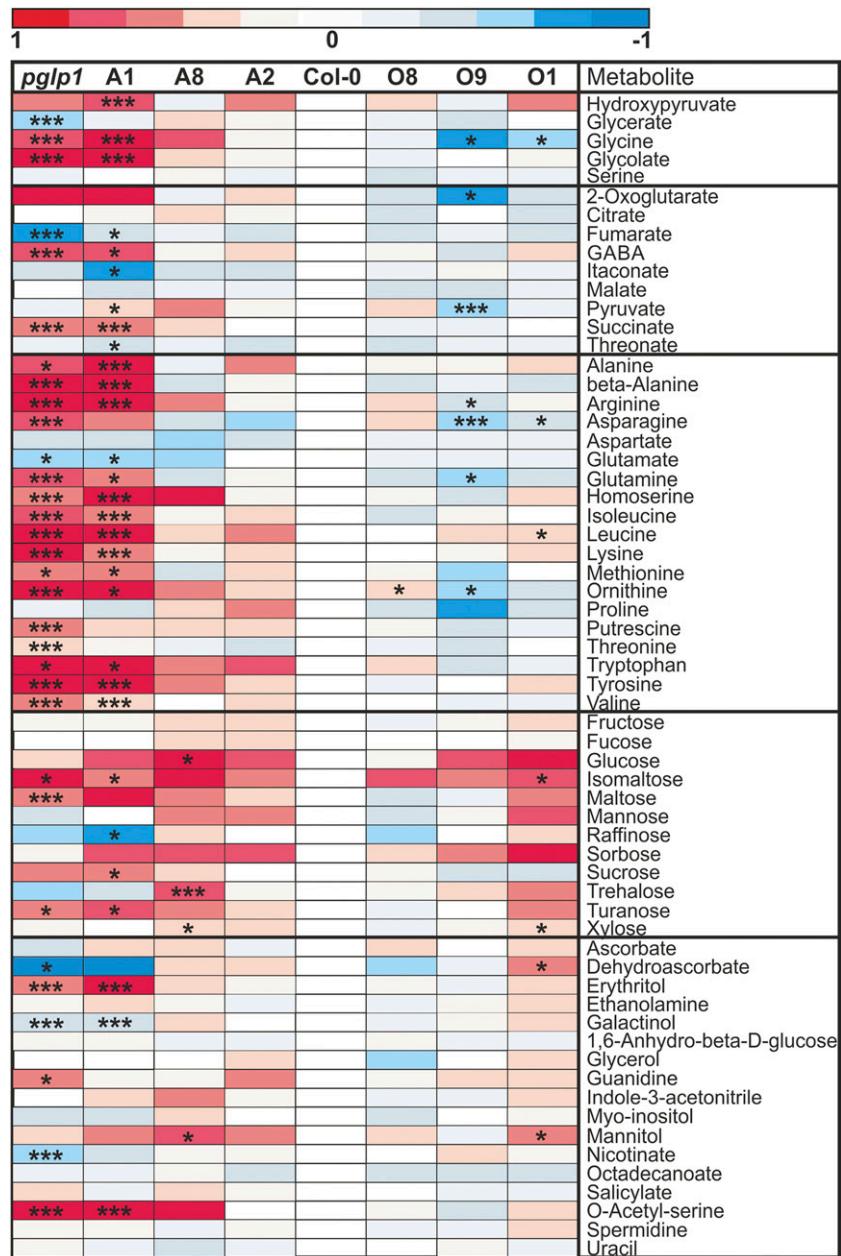
Figure 4. Heat Maps of Relative Metabolite Abundances at Normal Air (LC).

Plants were grown and leaf samples for metabolite analysis by GC-MS harvested exactly as described in Figure 3. Differences are color-coded as shown. Steady state metabolite contents are means ± sd relative to the wild-type mean value in LC (five different plants per genotype). Asterisks indicate values significantly different from the wild type in LC based on Student's t test (*P < 0.05; ***P < 0.01). See Supplemental Data Set 2 for the numerical data.

and LC, except massive alterations in *pglp1* and antisense line A1 (Figure 4; changes in HC are shown in Supplemental Figure 3). In these two lines, the increased levels of succinate and γ-aminobutyric acid (GABA) indicate alterations in the operation of the tricarboxylic acid cycle, including activation of the GABA shunt at very low PGLP1 activity. The levels of citrate and malate were similar in all lines, while fumarate levels were significantly lower in *pglp1* and line A1 relative to the wild type.

We also observed massive accumulation of a number of amino acids in these two lines, indicating enhanced protein degradation in the context of metabolic deregulation (Gibon et al., 2006; Usadel et al., 2008). The genetic intervention in antisense lines A2 and A8 as well as in the overexpressor plants altogether did not result in much significant metabolic variation in comparison with the wild type. However, it is remarkable that at least one of the overexpressor lines displayed lower contents of glycine,
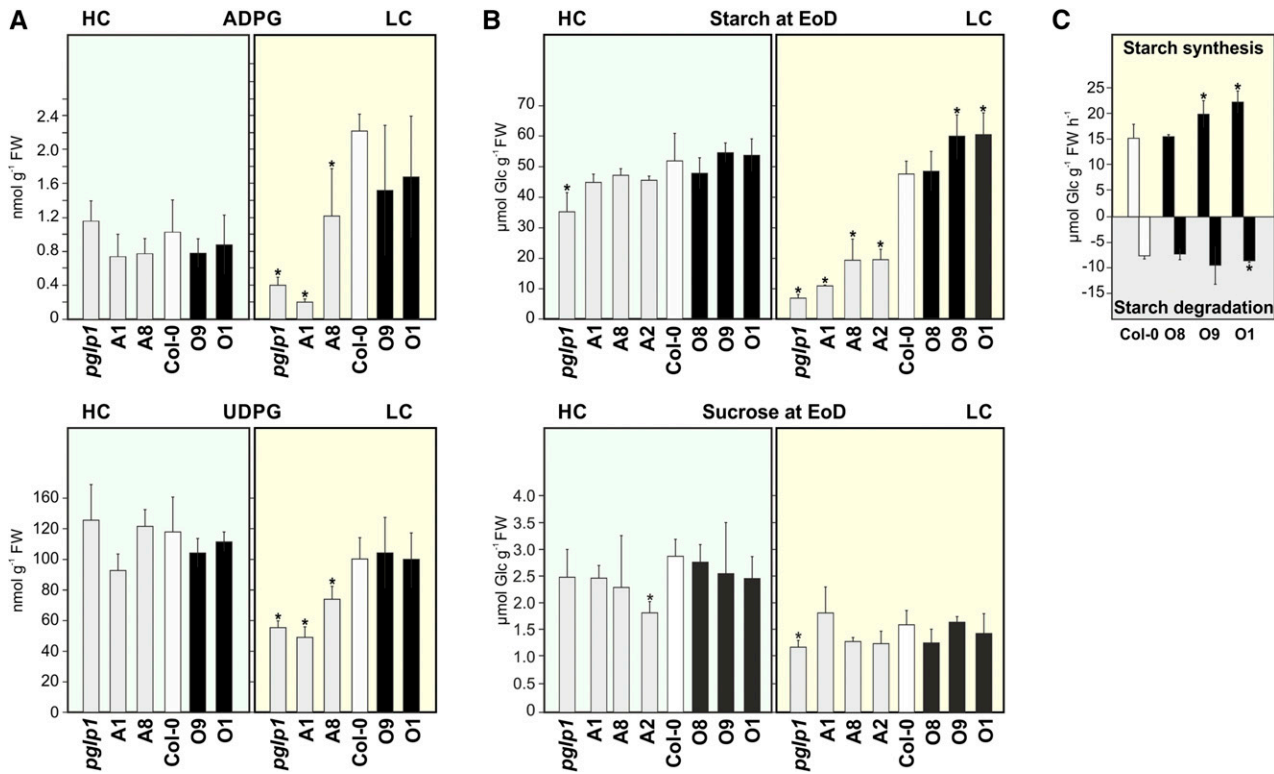
Figure 5. Leaf ADPG, UDPG, Starch, and Sucrose Contents in HC and LC and Starch Turnover.

(A) Contents of ADPG and UDPG at MoD. For details see legend to Figure 3.

(B) EoD leaf starch and sucrose contents in HC and 1 d after transfer to LC.

(C) Starch synthesis and degradation rates in LC. Columns represent means from at least four different plants. Asterisks indicate values significantly different from the wild type based on Student's t test (*P < 0.05).

2-oxoglutarate, pyruvate, asparagine, and glutamine (all significant in line O9). The LC levels of these metabolites followed the PGLP1 activity in an inverse direction (increased at higher and decreased at lower PGLP1 activity).

DISCUSSION

The CBC is at the heart of nearly all photosynthetic CO_2 fixation on Earth and linked to the photorespiratory pathway by the 2PG-producing oxygenation of RuBP, by the 3PGA produced from 2PG, and by the consumption of ATP and reducing power. Our study aimed to test the potential role of 2PG as a regulator of photosynthetic carbon metabolism. To this end, we analyzed the changes caused by the artificial modulation of the activity of PGLP1 and found that the data are consistent with 2PG acting as a metabolic regulator in vivo.

A key to understanding whether and, if so, how the enzymatic capacity of PGLP1 feeds back to the operation of the CBC itself was quantification of 2PG and CBC metabolites by LC-MS/MS. The antisense and overexpression lines showed a suitable graduation in leaf PGLP activity (Figure 1C) that significantly correlates with leaf 2PG contents. Excessive accumulation of 2PG such as that which occurs in low PGLP1 lines even under HC

conditions is clearly harmful (570-fold in *pglp1*, 26-fold in line A1, and 2-fold in line A8; photos in Figure 1D, numbers in Supplemental Data Set 1). In LC, the leaf 2PG content in antisense line A8 increased to be 250-fold higher than the wild-type value, too, whereas the values were significantly ~50% lower in the two examined overexpressors.

Assuming a stromal volume of 20 μL g^{-1} FW (Sharkey and Vanderveer, 1989), stromal 2PG concentrations in *pglp1* would be ~10 and 50 mM in HC and LC, respectively, and between 20 and 35 mM in the antisense lines A8 and A1 in LC. The estimated 2PG concentration of 0.1 mM in the wild type in LC would be well above the in vitro determined K_i of ~15 and ~35 μM of pea (Anderson, 1971) and Arabidopsis (Supplemental Figure 4) chloroplast TPI, respectively. A steady state concentration of ~0.1 mM 2PG in the chloroplast stroma therefore would be clearly relevant for TPI activity in vivo, which supports our hypothesis that PGLP1 activity and 2PG contents could be regulating variables in metabolic control. It is also interesting to note that line A1 shows a not very strong yet clear phenotypic alteration in HC in combination with wild-type-like starch accumulation and an estimated stromal 2PG concentration of ~0.5 mM. One may therefore speculate that the 2PG concentration range that is relevant for metabolic regulation may span the range from 0.05 to 0.5 mM, which corresponds to the

range of reported K_m values of PGLP (Husic and Tolbert, 1984; Hardy and Baldy, 1986; Seal and Rose, 1987; Norman and Colman, 1991).

Changes in most CBC metabolites were insignificant or inconsistent under HC, except for NADP, ADP, F6P, and, particularly, S7P. S7P displayed a significantly lower content in the antisense and in the overexpression lines (except for O9). This suggests that 2PG in addition to its effect on TPI may also inhibit sedoheptulose 1,7-bisphosphate phosphatase (SBPase). Inhibition of this enzyme by 2PG was also suggested by the fact that SBP levels are about 10-fold higher in LC than in HC for most genotypes except the two lines, A1 and *pglp1*, which accumulate 2PG even in HC. Potentially, this effect could be due to inhibition of SBPase by 2PG. We tested this hypothesis using recombinant Arabidopsis SBPase and found that 2PG inhibits SBPase with a K_i in the range of ∼10 μM (Supplemental Figure 5C). Considering the reported K_m of 13 μM SBP (Marques et al., 1987) in combination with the stromal 2PG concentration range discussed above, this would allow efficient regulation of SBPase activity by 2PG in vivo. SBPase is regulated by thioredoxin, is strongly pH and Mg^{2+} dependent, and is subject to efficient feedback inhibition by S7P (Schimkat et al., 1990; Raines et al., 2000), which makes the exact kinetic analysis of this enzyme difficult. While our experiments demonstrate that 2PG is a similarly powerful inhibitor of SBPase as it is of TPI, a future quantitative kinetic evaluation of the impact of 2PG on SBPase activity will clearly be necessary.

Interestingly, under photorespiratory conditions, we observed a largely similar "peak" pattern as for S7P under HC and LC for a number of other CBC metabolites including, for example, RuBP, 3PGA, DHAP, and SBP but not 2PG. This effect is likely due to a combination of at least two effects. First, alleviation of TPI and SBPase inhibition by 2PG may be the major effect on the high-PGLP1 (low 2PG) side, resulting in faster carbon flow through the CBC and lower steady state metabolite levels. Second, reduced levels of CBC metabolites due to massive sequestration of orthophosphate (P_i) in 2PG could increasingly dominate the response of CBC intermediates in the low-PGLP1 (high 2PG) side, especially in LC when 2PG accumulates to over 500 nmol g^{-1} FW, which exceeds the sum of P found in CB intermediates in wild-type plants. Superimposed on this metabolite deprivation would be inhibition of TPI and SBPase by 2PG and the resulting shifts in the balance between intermediates in the CBC. Depletion of stromal P_i, furthermore, potentially restricts ATP synthesis and is normally counteracted by allosteric activation (activation by 3PGA; inhibition by P_i) of ADPG pyrophosphorylase to enhance starch synthesis resulting in the release of P_i (Sowokinos and Preiss, 1982). This important regulatory mechanism may become less efficient or even nonoperational when P_i deprivation occurs due to the accumulation of 2PG, since the resulting inhibition of TPI and SBPase slows down starch synthesis.

Inhibition of SBPase by 2PG is an intriguing observation because this enzyme is the key point where carbon is committed to RuBP regeneration as opposed to starch synthesis. Indeed, the EoD leaf starch content of the different genotypes examined is positively correlated with the PGLP activity in LC and HC, including a stronger response in LC. By contrast, the leaf sucrose content remained essentially unaltered in two independent experiments using different detection methods. These measurements of sucrose

levels do not give direct information about the flux to sucrose. However, our suggestion that sucrose synthesis is not selectively inhibited in low PGLP1 lines is supported by an earlier report that the barley *pglp1* mutant RPr84/90 shows wild-type-like labeling of sucrose after $^{14}CO_2$ feeding (Hall et al., 1987). Moreover, the response of starch and sucrose to high 2PG resembles the observed linear decline in starch content in response to reductions in SBPase activity in combination with a nearly unaltered sucrose level in antisense tobacco plants (Raines et al., 2000; Ölçer et al., 2001). However, it should be stressed that whereas less accumulation at a given time point demonstrates that starch is accumulating slower, unaltered sucrose could mean that it is made and exported with the same or higher or lower rates. Furthermore, it is possible that the lower rate of starch accumulation is in part due to increased degradation, which increases even in the light when CBC metabolites are depleted (Weise et al., 2006) as they are in the low-PGLP1 lines. Flux studies will be necessary to definitively answer this question, but it is interesting that CBC antisense transgenic plants display similar features (Koßmann et al., 1994) and that maintaining the daytime flux of carbon to sucrose at the expense of starch synthesis is considered a general response to reduced CBC activity (Raines et al., 2000).

Daytime accumulation of transitory starch in the mesophyll is necessary for healthy growth and consumes 30 to 50% of photoassimilates in Arabidopsis leaves (Stitt and Zeeman, 2012). In the guard cells, starch accumulation and mobilization are important for stomatal turgor generation and opening (Prasch et al., 2015; Horrer et al., 2016). In drought conditions, starch is rapidly mobilized via a pathway using α-AMYLASE3 and β-AMYLASE1 (Thalmann et al., 2016; Zanella et al., 2016). We did not assess starch accumulation in guard cells but would expect that altered 2PG contents would affect photosynthetic metabolism in these cells in a similar way as it does in the mesophyll. It is noteworthy that there were significantly decreased values for g_s in all three *PGLP1* antisense lines after transfer to LC and significantly increased values in all three overexpressor lines at 40% O_2 (Table 2). Stomatal conductance is often correlated with the mesophyll diffusion conductance g_m (Flexas et al., 2012), and a multispecies analysis of quantitative photosynthesis and metabolome data suggested coregulation of g_s and g_m (Gago et al., 2016). However, this is an emerging field and as such is not yet fully explored. Eisenhut et al. (2017) recently reported that the transcriptional response of *pglp1* during acclimation to LC includes drought stress-related genes, suggesting that an increase in capacity of photorespiratory metabolism may be a prerequisite for rapid physiological acclimation to a reduction in CO_2 availability. Our data are in agreement with this hypothesis. It is well possible that an artificially elevated content of 2PG in guard cells wrongly signals reduced CO_2 availability, mimicking drought stress. In a wild-type context, drought stress alters the internal CO_2/O_2 concentration ratio, likely resulting in higher 2PG levels in guard cell chloroplasts. This would restrict the accumulation of transitory starch that is available for mobilization at the start of the next day for stomata opening (Horrer et al., 2016).

Moderate decreases (lines A2 and A8) or increases (all overexpressor lines) in PGLP1 activity have little effect on the relative steady state abundances of most of the examined 62 non-phosphorylated indicator metabolites of central metabolism in

LC (Figure 4) and, as would be expected, even less impact in HC (Supplemental Figure 3). The few changes include a significant negative correlation between PGLP activity and glycine contents over all genotypes in HC and LC and lower contents of asparagine in the overexpressor lines O1 and particularly O9 under LC. These changes indicate alleviated flux through the photorespiratory pathway, maybe in combination with increased usage of asparagine as an additional donor of amino groups for glyoxylate amination (Zhang et al., 2013; Modde et al., 2017). By contrast, the antisense line A1 (~9% PGLP1 activity) and the knockout mutant *pglp1* show many distinct changes already in HC and even more in LC. It is not intuitively clear which pathway is responsible for the glycolate accumulation in these two lines. Significant rates of nonphotorespiratory glycolate production, for example, by transketolase from fructose 6-phosphate (Christen and Gasser, 1980), are considered unlikely to occur in vivo (Somerville and Ogren, 1979). There may be alternative routes, however, including the possibility that at the very high stromal concentration of 2PG (~50 mM in LC as roughly calculated above) a fraction flows out of the chloroplast, maybe in an unknown side reaction of a translocator, and is converted to glycolate in the cytosol by PGLP2 (Schwarte and Bauwe, 2007) or indeed in any extraplastidial compartment by nonspecific phosphatases. Another prominent feature of these two lines is the accumulation, for example, of branched-chain amino acids, guanidine and ornithine, which is already visible in HC and indicates a metabolic disorder related to enhanced protein degradation (Gibon et al., 2006; Usadel et al., 2008; Nelson et al., 2014; Hildebrandt et al., 2015). Accumulation of GABA has often been observed when plants are exposed to abiotic or biotic stresses but its role in metabolism and signaling is not yet fully understood (Häusler et al., 2014). In *pglp1* and line A1 in LC, GABA accumulation is accompanied by glutamate deprivation. This coincidence may indicate conversion of glutamate, some of which could directly or indirectly via lysine arise from protein degradation, to GABA as a component of stress-induced metabolic rearrangements (Fait et al., 2008). All these massive changes occur exclusively in *pglp1* and in line A1. Hence, overall, the GC-MS metabolome data demonstrate that a moderately lower or higher PGLP1 activity does not induce a systemic metabolic response but rather exerts specific effects on photosynthetic carbon metabolism.

Lower PGLP1 activity had a considerable negative impact on photosynthesis and plant growth (Figures 1 and 2). In the overexpressor lines, by contrast, changes in gas exchange parameters were detectable to a statistically significant magnitude only under the high photorespiratory pressure of 40% O_2 (Table 2). Under this condition, net photosynthesis was significantly increased in all three lines, and Γ_{40} is lower in the line with the highest PGLP activity. Γ_{21}^* remained unchanged, indicating an unaltered carboxylation-to-oxygenation ratio. Nighttime respiration was also significantly increased in this line, possibly corresponding to the higher starch content. These changes coincide with slightly though significantly improved growth (four parameters in the two overexpressor lines with the highest PGLP1 activity, larger rosette diameter in line O8; Table 1). Collectively, it appears that more PGLP1 and in turn a lower steady state concentration of 2PG facilitate photosynthetic gas exchange and growth to some

extent, particularly under high photorespiratory pressure. We assume that the moderate growth improvement is due to higher carbon flow through the CBC (due to alleviated 2PG inhibition of TPI and SBPase) in combination with a somewhat higher accumulation of transitory starch, supporting growth at night more efficiently. The finding that increased expression of SBPase can stimulate photosynthesis (Lefebvre et al., 2005) makes it plausible that CBC flux may be stimulated in PGLP1 overexpressors by alleviating the inhibition of SBPase via a decrease in 2PG.

In summary, we conclude that 2PG is not simply one of many photorespiratory metabolites. Changes in the activity of the photorespiratory enzyme PGLP1, and in turn stromal 2PG contents, readjust operation of photosynthetic carbon metabolism, particularly carbon allocation to RuBP regeneration and starch synthesis. This occurs via inhibition of two key CBC enzymes, TPI and SBPase, and likely represents a regulatory feedback loop from the photorespiratory pathway to the CBC that in concert with other regulation adjusts carbon flow through the CBC and carbon partitioning between starch synthesis and the regeneration of RuBP. Hence, regulation by 2PG appears to be one of the mechanisms by which plants can adapt in the short term to the everchanging environment, such as intermittent CO_2 deprivation at high light intensity or temperature. In light of its suggested role for the low-CO_2 acclimation of cyanobacteria (Haimovich-Dayan et al., 2015), 2PG signaling could actually be an evolutionarily conserved regulatory mechanism. From an experimental point of view, it is long known and useful that photorespiratory mutants can be grown and propagated in air enriched to 1% CO_2, but this should not be taken to imply the complete absence of photorespiration under these conditions.

METHODS

Plants and Plant Growth Conditions

Arabidopsis thaliana ecotype Columbia (Col-0) was used as wild-type control and to generate *PGLP* antisense and overexpression lines. The homozygous T-DNA insertional line of *PGLP1* (*pglp1*) described previously (Schwarte and Bauwe, 2007) was used as the knockout control and for molecular complementation. Prior to cultivation, seeds were sterilized with chloric acid, sown on soil, and incubated at 4°C to break dormancy for at least 2 d. Except stated otherwise, plants were grown to stage 5.1 according to Boyes et al. (2001) in controlled environment chambers (Percival; 10-h photoperiod, 20/18°C, ~120 µmol m^{-2} s^{-1} irradiance) at 0.04% (LC, normal air) or 1% (HC, elevated CO_2) µL L^{-1} CO_2) on a 4:1 mixture of soil (Type Mini Tray; Einheitserdewerk) and vermiculite, and regularly watered with 0.2% Wuxal liquid fertilizer (Aglukon) as the standard.

cDNA Cloning, Complementation, and Expression

To generate *PGLP1* complementation and antisense lines, the entire coding sequence (1089 bp) was PCR-amplified from Arabidopsis cDNA using oligonucleotides P518 and P519 for complementation and P520 and P521 for the antisense construct (all oligonucleotide sequences in Supplemental Table 2). The resulting fragments (*compPGLP* and *antiPGLP*) were ligated into vector pGEM-T (Invitrogen) and verified by sequencing. Fragments (*compPGLP*, *Sac*I-*Eco*RI; *antiPGLP*, *Sac*I-*Bam*HI) were excised and ligated between the CaMV 35S promoter and the CaMV poly(A) site of the pGreen 35S-CaMV cassette (http://www.pgreen.ac.uk/). The resulting fusions (*35Spro:compPGLP:CaMV* and *35Spro:antiPGLP:CaMV*) were further

excised via *Eco*RV and ligated into the binary plant transformation vector pGREEN0229. For overexpression, the entire coding region of *PGLP* was amplified via oligonucleotides P656 and P673, fused to the 35S terminator, and introduced into pGREEN0229 under the control of the light regulated, mesophyll-specific *ST-LS1* promoter, as used previously (Timm et al., 2012a, 2015). The resulting constructs (Supplemental Figure 1) were introduced into *Agrobacterium tumefaciens* strain GV3101 and used for transformation (Clough and Bent, 1998) of the Arabidopsis *pglp1*-deficient mutant or the wild type. The resulting phosphinotricine (Basta) resistant individuals were verified and preselected according their leaf PGLP1 content by immunoblotting, and stable T4 lines from three independent lines (designated as C1–C3 for complementation, A1, A2, and A8 for antisense, and O1, O8, and O9 for overexpression) were used for subsequent analysis.

Validation of Transgenic Lines, RT-qPCR, and Immunological Studies

The integration of the *PGLP1* complementation, antisense, and overexpression construct into the genome was verified via PCR from leaf DNA (1 min at 94°C, 1 min at 58°C, and 1.5 min at 72°C, 35 cycles) with primers specific for the 35S (P246) or the *ST-LS*1 promoter (P278) and the CaMV terminator (P363), respectively (Supplemental Figure 1). The *S16* gene (1 min at 94°C, 1 min at 58°C, and 30 s at 72°C; 35 cycles) served as the internal control. The functionality of the integrated antisense and overexpression constructs was first verified by RT-qPCR using 2.5 μg leaf RNA for cDNA synthesis (Nucleospin RNA plant kit, Macherey-Nagel; RevertAid cDNA synthesis kit, MBI Fermentas) and the oligonucleotide combination P393 and P394, yielding a 328-bp PCR product for the *PGLP* transcript. Prior to RT-qPCR analysis, cDNA amounts were calibrated according to signals from 432-bp fragments of the constitutively expressed 40S ribosomal protein *S16* gene, with oligonucleotides P444 and P445. Detection and normalization of *PGLP1* expression were performed as described previously (Timm et al., 2013), and mRNA amounts of *PGM*, *PGI*, *TPI*, and *SBPase* were quantified accordingly. Plant material (~100 mg leaf tissue pooled from three different plants per genotype) for nucleic acid isolation was harvested at MoD (after 5 h illumination). Complementation, antisense repression, and overexpression of the transgene were further verified by immunoblotting. Briefly, protein extracts from ~100 mg leaf tissue (at least two different individuals per genotype) were separated by SDS-PAGE followed by immunoblotting according to standard protocols. Complementation, antisense repression, and overexpression was detected using specific antibodies against PGLP1 and against HPR1 (Timm et al., 2013) as a calibration control.

Recombinant Enzymes

Arabidopsis whole-leaf cDNA prepared as above was PCR amplified with the primer pair P894 (sense) and P895 (antisense) for the SBPase CDS and the primer pair P749 (sense) and P750 (antisense) for the TPI CDS. The resulting fragments, which were flanked by restriction sites (*Nhe*I/*Eco*RI for SBPase and *Eco*RI/*Xho*I for TPI), were ligated into vector pGEM-T Easy (Promega) for sequence confirmation (Seqlab). By using the introduced restriction sites, the CDSs were excised and in-frame ligated into the expression vector pET28b (Merck) for SBPase or pASK-IBA6 (IBA Lifesciences) for TPI. SBPase expression and purification was performed exactly as specified by Dunford et al. (1998). TPI expression was performed in *Escherichia coli* BL21 in a total volume of 500 mL LB medium at 37°C (200 rpm). For the induction of expression, the culture was cooled to 20°C and 200 μg L^{-1} anhydrotetracycline added. After 12 h (200 rpm), cells were harvested (10 min, 8000g, 4°C), resuspended in ice-cold 20 mM sodium phosphate (pH 7.8), and ultrasonified on ice (six 30-s bursts at 50 W). After centrifugation (20,000g, 20 min, 4°C), the recombinant TPI

was affinity-purified on a Strep-Tactin matrix (IBA) and rebuffered in 100 mM Tris-HCl (pH 8.0) by passage through PD-10 columns (GE Healthcare).

Enzyme Measurements

PGLP activity in leaf extracts of at least five different individuals per genotype was determined according to Somerville and Ogren (1979). The total reaction volume of 2 mL contained 5 mM HEPES (pH 6.3), 40 mM sodium cacodylate, 5 mM citrate, 5 mM ZnSO$_4$, 0.5 mM EDTA, and 200 μg protein. The reaction was initiated at 25°C by adding 2 mM 2PG, and, at 0, 2, 4, 6, 8, and 10 min, 300 μL aliquots were mixed with 700 μL of acid molybdate reagent [1:6 mixture of 10% (w/v) ascorbate and 0.42% (w/v) $(NH_4)_6Mo_7O_{24} \times 4 H_2O$ in 1 N sulfuric acid] to stop enzymatic activity. The samples were incubated at 45°C for 20 min and the released phosphate photometrically determined at 820 nm (Ames, 1966).

SBPase activity was measured in an assay modified from Dunford et al. (1998). Reaction mixtures (total volume of 384 μL without enzyme) contained 5 mM Tris-HCl (pH 8.2), 1 mM MgCl$_2$, 0.1 mM EDTA, 10 mM DTT, 130 μM SBP (Organix), and no 2PG ($n = 2$) or 130 μM 2PG ($n = 4$; Sigma-Aldrich). For each mixture, time 0 was obtained by taking 48 μL, adding 1 μg (2 μL) of SBPase (previously heated at 100°C for 3 min) and mixing with 250 μL of cold chloroform/methanol (v:v, 3:7). After addition of SBPase to the remaining reaction mixture (7 μg, 14 μL), incubation was performed at 25°C. At 2, 4, 6, and 8 min, 50 μL of the mixture were removed and treated as above to stop enzymatic activity and kept on ice until all samples were processed. After lyophilization, samples were resuspended in 250 μL water, diluted 1:2, and S7P quantified by LC-MS/MS according to Arrivault et al. (2009). The K$_i$ was estimated from the respective standard equation for competitive enzyme inhibition using the following parameters: 130 μM SBP, 130 μM 2PG, and K_m (SBP) = 13 μM (Marques et al., 1987).

TPI activity was routinely assayed at 25°C in a total volume of 1 mL containing 100 mM Tris-HCl (pH 8.0), 0.2 mM NADH, and 2 units glyceraldehyde 3-phosphate (G3P) dehydrogenase. The reaction was initiated by adding 0.1 mM G3P. For the determination of the K$_i$ for 2PG, TPI activity was measured at 0.2, 0.4, 0.8, 2, and 4 mM G3P in the presence of 0, 15, and 75 μM 2PG. All measurements were performed in triplicate.

Growth Parameters

Growth parameters were determined from plants at stage 5.1 (about 8 weeks after sowing), grown under standard conditions (10-h photoperiod, 20/18°C day/night, ~120 μmol m^{-2} s^{-1} photosynthetically active radiation, ~70% relative humidity, 0.04% CO$_2$). Rosette diameters (longest possible distance) and total leaf number of 20 different plants per genotype were determined. The same plants were used to measure the shoot fresh and dry weight (105°C, overnight).

Gas Exchange and Chlorophyll *a* Fluorescence

Standard gas exchange measurements were essentially performed as described by Timm et al. (2015). *PGLP1* antisense plants were first grown under elevated CO$_2$ conditions (1% CO$_2$, HC) to growth stage 5.1 (Boyes et al., 2001) and then transferred to normal air (0.04% CO$_2$, LC) with otherwise equal conditions. Net CO$_2$ uptake rates (A) and CO$_2$ compensation points (Γ) were determined from five different HC-grown plants per genotype at days 0 (HC control), 1, 3, 5, and 7 after the transfer to LC. O$_2$ inhibition of A was calculated as % inhibition = 100(A$_{21}$ − A$_{40}$)/A$_{21}$.

PGLP1 complementation and overexpression lines were grown in normal air to growth stage 5.1. Different O$_2$ concentrations were generated using the gas mixing system GMS600 (QCAL Messtechnik). For the determination of in vivo chlorophyll *a* fluorescence, we used an Imaging Pulse Amplitude Modulation fluorometer (M-Series; Walz) and dark-adapted

plants (10 min) at growth stage 5.1. The measurements were performed as described previously with at least five different plants per genotype (Timm et al., 2012b).

Metabolite Analysis

For GC-MS metabolite analysis (five different plants per genotype), we took samples at MoD (after 5 h light) under HC and the next day after 5 h exposure to LC conditions in the light. Leaf samples of 50 mg were harvested from plants at growth stage 5.1 (Boyes et al., 2001), immediately frozen in liquid nitrogen, and stored at −80°C until analysis. The procedures for metabolite extraction, derivatization, and analysis were as described previously (Lisec et al., 2006). For LC-MS/MS analysis (five different plants per genotype), we essentially used the same set of plants, sampling time points, and growth conditions as above. For metabolite determinations, 20 mg of leaf tissue were used and processed exactly as described by Arrivault et al. (2009, 2015) with the addition of quantification of 2PG (Arrivault et al., 2017). 3-PGA was quantified from 100 mg leaves using the enzymatic assay described by Gibon et al. (2002). Starch and sucrose were measured enzymatically according to Cross et al. (2006) from ∼25 mg leaf tissue harvested at EoD (for *pglp1* and the antisense lines in HC and 1 d after transfer to LC) from five plants per genotype. The rates of synthesis and degradation were determined as linear regression slopes calculated from four daytime (2-h intervals) and four nighttime values (4-h intervals) as described by Lu et al. (2005).

Statistical Analysis

Statistical significance of differences was tested using the two-tailed Student's *t* test algorithm incorporated into Microsoft Excel 10.0 (Microsoft). Correlation analysis was performed with Spearman's rank order test in SPSS Statistics 22 (IBM). The term significant is used here for differences or correlations confirmed at *P < 0.05 or better.

Accession Numbers

Sequence data from this article can be found in the GenBank/EMBL data libraries under the following accession numbers: At5g36700 (*PGLP1*), At5g47760 (*PGLP2*), At1g68010 (*HPR1*), At5g51820 (PGM), At4g24620 (*PGI*), At3g55800 (*SBPase*), At2g21170 (plastidic *TPI*), and At2g09990 (40S ribosomal protein *S16*).

Supplemental Data

Supplemental Figure 1. Constructs used and genotyping of transgenic lines.

Supplemental Figure 2. Genetic complementation of the *pglp1* T-DNA insertional mutant.

Supplemental Figure 3. Heat maps of relative metabolite abundances at 1% CO₂.

Supplemental Figure 4. Inhibition of Arabidopsis TPI by 2PG.

Supplemental Figure 5. Inhibition of Arabidopsis SBPase by 2PG.

Supplemental Figure 6. Abundances of transcripts for PGM, PGI, SBPase, and TPI.

Supplemental Table 1. Spearman rank-order correlation coefficients.

Supplemental Table 2. Oligonucleotides.

Supplemental Data Set 1. Metabolite contents as determined by LC-MS/MS.

Supplemental Data Set 2. Metabolite contents as determined by GC-MS.

AUTHOR CONTRIBUTIONS

A.R.F. and H.B. conceived the project. A.R.F., H.B., and S.T. designed and supervised the experiments. A.F., F.F., S.A., and S.T. performed the experiments and analyzed data. F.F. and S.T. drafted the article. H.B. wrote the manuscript with additions and revisions by A.R.F., M.S., S.A., and S.T.

REFERENCES

Ames, B.N. (1966). Assay of inorganic phosphate, total phosphate and phosphatases. In Methods in Enzymology: Complex Carbohydrates, E.F. Neufeld and V. Ginsburg, eds (New York: Academic Press), pp. 115–118.

Anderson, L.E. (1971). Chloroplast and cytoplasmic enzymes. II. Pea leaf triose phosphate isomerases. Biochim. Biophys. Acta **235:** 237–244.

Arrivault, S., Guenther, M., Ivakov, A., Feil, R., Vosloh, D., van Dongen, J.T., Sulpice, R., and Stitt, M. (2009). Use of reverse-phase liquid chromatography, linked to tandem mass spectrometry, to profile the Calvin cycle and other metabolic intermediates in Arabidopsis rosettes at different carbon dioxide concentrations. Plant J. **59:** 826–839.

Arrivault, S., Guenther, M., Fry, S.C., Fuenfgeld, M.M.F.F., Veyel, D., Mettler-Altmann, T., Stitt, M., and Lunn, J.E. (2015). Synthesis and use of stable-isotope-labeled internal standards for quantification of phosphorylated metabolites by LC-MS/MS. Anal. Chem. **87:** 6896–6904.

Arrivault, S., Obata, T., Szecówka, M., Mengin, V., Guenther, M., Hoehne, M., Fernie, A.R., and Stitt, M. (2017). Metabolite pools and carbon flow during C₄ photosynthesis in maize: ¹³CO₂ labeling kinetics and cell type fractionation. J. Exp. Bot. **68:** 283–298.

Beaudoin, G.A., and Hanson, A.D. (2016). A guardian angel phosphatase for mainline carbon metabolism. Trends Biochem. Sci. **41:** 893–894.

Betti, M., Bauwe, H., Busch, F.A., Fernie, A.R., Keech, O., Levey, M., Ort, D.R., Parry, M.A., Sage, R., Timm, S., Walker, B., and Weber, A.P. (2016). Manipulating photorespiration to increase plant productivity: recent advances and perspectives for crop improvement. J. Exp. Bot. **67:** 2977–2988.

Bowes, G., Ogren, W.L., and Hageman, R.H. (1971). Phosphoglycolate production catalyzed by ribulose diphosphate carboxylase. Biochem. Biophys. Res. Commun. **45:** 716–722.

Boyes, D.C., Zayed, A.M., Ascenzi, R., McCaskill, A.J., Hoffman, N.E., Davis, K.R., and Görlach, J. (2001). Growth stage-based phenotypic analysis of Arabidopsis: a model for high throughput functional genomics in plants. Plant Cell **13:** 1499–1510.

Christen, P., and Gasser, A. (1980). Production of glycolate by oxidation of the 1,2-dihydroxyethyl-thamin-diphosphate intermediate

of transketolase with hexacyanoferrate(III) or H_2O_2. Eur. J. Biochem. **107:** 73–77.

Clough, S.J., and Bent, A.F. (1998). Floral dip: a simplified method for *Agrobacterium*-mediated transformation of *Arabidopsis thaliana*. Plant J. **16:** 735–743.

Collard, F., et al. (2016). A conserved phosphatase destroys toxic glycolytic side products in mammals and yeast. Nat. Chem. Biol. **12:** 601–607.

Cross, J.M., von Korff, M., Altmann, T., Bartzetko, L., Sulpice, R., Gibon, Y., Palacios, N., and Stitt, M. (2006). Variation of enzyme activities and metabolite levels in 24 Arabidopsis accessions growing in carbon-limited conditions. Plant Physiol. **142:** 1574–1588.

Dunford, R.P., Catley, M.A., Raines, C.A., Lloyd, J.C., and Dyer, T.A. (1998). Purification of active chloroplast sedoheptulose-1,7-bisphosphatase expressed in *Escherichia coli*. Protein Expr. Purif. **14:** 139–145.

Eisenhut, M., Bräutigam, A., Timm, S., Florian, A., Tohge, T., Fernie, A.R., Bauwe, H., and Weber, A.P.M. (2017). Photorespiration is crucial for dynamic response of photosynthetic metabolism and stomatal movement to altered CO_2 availability. Mol. Plant **10:** 47–61.

Fait, A., Fromm, H., Walter, D., Galili, G., and Fernie, A.R. (2008). Highway or byway: the metabolic role of the GABA shunt in plants. Trends Plant Sci. **13:** 14–19.

Flexas, J., et al. (2012). Mesophyll diffusion conductance to CO_2: an unappreciated central player in photosynthesis. Plant Sci. **193-194:** 70–84.

Gago, J., Daloso, Dde.M., Figueroa, C.M., Flexas, J., Fernie, A.R., and Nikoloski, Z. (2016). Relationships of leaf net photosynthesis, stomatal conductance, and mesophyll conductance to primary metabolism: A multispecies meta-analysis approach. Plant Physiol. **171:** 265–279.

Gibon, Y., Vigeolas, H., Tiessen, A., Geigenberger, P., and Stitt, M. (2002). Sensitive and high throughput metabolite assays for inorganic pyrophosphate, ADPGlc, nucleotide phosphates, and glycolytic intermediates based on a novel enzymic cycling system. Plant J. **30:** 221–235.

Gibon, Y., Usadel, B., Blaesing, O.E., Kamlage, B., Hoehne, M., Trethewey, R., and Stitt, M. (2006). Integration of metabolite with transcript and enzyme activity profiling during diurnal cycles in Arabidopsis rosettes. Genome Biol. **7:** R76.

Hagemann, M., Kern, R., Maurino, V.G., Hanson, D.T., Weber, A.P., Sage, R.F., and Bauwe, H. (2016). Evolution of photorespiration from cyanobacteria to land plants, considering protein phylogenies and acquisition of carbon concentrating mechanisms. J. Exp. Bot. **67:** 2963–2976.

Haimovich-Dayan, M., Lieman-Hurwitz, J., Orf, I., Hagemann, M., and Kaplan, A. (2015). Does 2-phosphoglycolate serve as an internal signal molecule of inorganic carbon deprivation in the cyanobacterium *Synechocystis* sp. PCC 6803? Environ. Microbiol. **17:** 1794–1804.

Hall, N.P., Kendall, A.C., Lea, P.J., Turner, J.C., and Wallsgrove, R.M. (1987). Characteristics of a photorespiratory mutant of barley (*Hordeum vulgare* L.) deficient in phosphogly collate phosphatase. Photosynth. Res. **11:** 89–96.

Hardy, P., and Baldy, P. (1986). Corn phosphoglycolate phosphatase: purification and properties. Planta **168:** 245–252.

Häusler, R.E., Ludewig, F., and Krueger, S. (2014). Amino acids–a life between metabolism and signaling. Plant Sci. **229:** 225–237.

Heineke, D., Bykova, N., Gardeström, P., and Bauwe, H. (2001). Metabolic response of potato plants to an antisense reduction of the P-protein of glycine decarboxylase. Planta **212:** 880–887.

Hildebrandt, T.M., Nunes Nesi, A., Araújo, W.L., and Braun, H.P. (2015). Amino acid catabolism in plants. Mol. Plant **8:** 1563–1579.

Horrer, D., Flütsch, S., Pazmino, D., Matthews, J.S., Thalmann, M., Nigro, A., Leonhardt, N., Lawson, T., and Santelia, D. (2016). Blue light induces a distinct starch degradation pathway in guard cells for stomatal opening. Curr. Biol. **26:** 362–370.

Husic, H.D., and Tolbert, N.E. (1984). Anion and divalent cation activation of phosphoglycolate phosphatase from leaves. Arch. Biochem. Biophys. **229:** 64–72.

Kelly, G.J., and Latzko, E. (1976). Inhibition of spinach-leaf phosphofructokinase by 2-phosphoglycollate. FEBS Lett. **68:** 55–58.

Knight, J., Hinsdale, M., and Holmes, R. (2012). Glycolate and 2-phosphoglycolate content of tissues measured by ion chromatography coupled to mass spectrometry. Anal. Biochem. **421:** 121–124.

Koßmann, J., Sonnewald, U., and Willmitzer, L. (1994). Reduction of the chloroplastic fructose-1,6-bisphosphatase in transgenic potato plants impairs photosynthesis and plant growth. Plant J. **6:** 637–650.

Lefebvre, S., Lawson, T., Zakhleniuk, O.V., Lloyd, J.C., Raines, C.A., and Fryer, M. (2005). Increased sedoheptulose-1,7-bisphosphatase activity in transgenic tobacco plants stimulates photosynthesis and growth from an early stage in development. Plant Physiol. **138:** 451–460. Erratum. Plant Physiol. 138: 1174.

Linster, C.L., Van Schaftingen, E., and Hanson, A.D. (2013). Metabolite damage and its repair or pre-emption. Nat. Chem. Biol. **9:** 72–80.

Lisec, J., Schauer, N., Kopka, J., Willmitzer, L., and Fernie, A.R. (2006). Gas chromatography mass spectrometry-based metabolite profiling in plants. Nat. Protoc. **1:** 387–396.

Lu, Y., Gehan, J.P., and Sharkey, T.D. (2005). Daylength and circadian effects on starch degradation and maltose metabolism. Plant Physiol. **138:** 2280–2291.

Marques, I.A., Ford, D.M., Muschinek, G., and Anderson, L.E. (1987). Photosynthetic carbon metabolism in isolated pea chloroplasts: metabolite levels and enzyme activities. Arch. Biochem. Biophys. **252:** 458–466.

Modde, K., Timm, S., Florian, A., Michl, K., Fernie, A.R., and Bauwe, H. (2017). High serine:glyoxylate aminotransferase activity lowers leaf daytime serine levels, inducing the phosphoserine pathway in Arabidopsis. J. Exp. Bot. **68:** 643–656.

Mugabo, Y., et al. (2016). Identification of a mammalian glycerol-3-phosphate phosphatase: Role in metabolism and signaling in pancreatic β-cells and hepatocytes. Proc. Natl. Acad. Sci. USA **113:** E430–E439.

Nelson, C.J., Li, L., and Millar, A.H. (2014). Quantitative analysis of protein turnover in plants. Proteomics **14:** 579–592.

Norman, E.G., and Colman, B. (1991). Purification and characterization of phosphoglycolate phosphatase from the cyanobacterium *Coccochloris peniocystis*. Plant Physiol. **95:** 693–698.

Olçer, H., Lloyd, J.C., and Raines, C.A. (2001). Photosynthetic capacity is differentially affected by reductions in sedoheptulose-1,7-bisphosphatase activity during leaf development in transgenic tobacco plants. Plant Physiol. **125:** 982–989.

Ort, D.R., et al. (2015). Redesigning photosynthesis to sustainably meet global food and bioenergy demand. Proc. Natl. Acad. Sci. USA **112:** 8529–8536.

Prasch, C.M., Ott, K.V., Bauer, H., Ache, P., Hedrich, R., and Sonnewald, U. (2015). β-Amylase1 mutant Arabidopsis plants show drought tolerance due to reduced starch breakdown in guard cells. J. Exp. Bot. **66:** 6059–6067.

Raines, C.A., Harrison, E.P., Ölçer, H., and Lloyd, J.C. (2000). Investigating the role of the thiol-regulated enzyme sedoheptulose-1,7-bisphosphatase in the control of photosynthesis. Physiol. Plant. **110:** 303–308.

Rose, Z.B., and Liebowitz, J. (1970). 2,3-Diphosphoglycerate phosphatase from human erythrocytes. General properties and activation by anions. J. Biol. Chem. **245:** 3232–3241.

Rose, Z.B., Grove, D.S., and Seal, S.N. (1986). Mechanism of activation by anions of phosphoglycolate phosphatases from spinach and human red blood cells. J. Biol. Chem. 261: 10996–11002.

Sasaki, H., Fujii, S., Yoshizaki, Y., Nakashima, K., and Kaneko, T. (1987). Phosphoglycolate synthesis by human erythrocyte pyruvate kinase. Acta Haematol. 77: 83–86.

Sasaki, R., Ikura, K., Sugimoto, E., and Chiba, H. (1975). Purification of bisphosphoglyceromutase, 2,3-bisphosphoglycerate phosphatase and phosphoglyceromutase from human erythrocytes. Eur. J. Biochem. 50: 581–593.

Schimkat, D., Heineke, D., and Heldt, H.W. (1990). Regulation of sedoheptulose-1,7-bisphosphatase by sedoheptulose-7-phosphate and glycerate, and of fructose-1,6-bisphosphatase by glycerate in spinach chloroplasts. Planta 181: 97–103.

Schwarte, S., and Bauwe, H. (2007). Identification of the photorespiratory 2-phosphoglycolate phosphatase, PGLP1, in Arabidopsis. Plant Physiol. 144: 1580–1586.

Seal, S.N., and Rose, Z.B. (1987). Characterization of a phosphoenzyme intermediate in the reaction of phosphoglycolate phosphatase. J. Biol. Chem. 262: 13496–13500.

Seifried, A., Bergeron, A., Boivin, B., and Gohla, A. (2016). Reversible oxidation controls the activity and oligomeric state of the mammalian phosphoglycolate phosphatase AUM. Free Radic. Biol. Med. 97: 75–84.

Sharkey, T.D., and Vanderveer, P.J. (1989). Stromal phosphate concentration is low during feedback limited photosynthesis. Plant Physiol. 91: 679–684.

Somerville, C.R., and Ogren, W.L. (1979). A phosphoglycolate phosphatase-deficient mutant of Arabidopsis. Nature 280: 833–836.

Sowokinos, J.R., and Preiss, J. (1982). Pyrophosphorylases in Solanum tuberosum: III. Purification, physical, and catalytic properties of ADP-glucose pyrophosphorylase in potatoes. Plant Physiol. 69: 1459–1466.

Stitt, M., and Zeeman, S.C. (2012). Starch turnover: pathways, regulation and role in growth. Curr. Opin. Plant Biol. 15: 282–292.

Stitt, M., Lunn, J., and Usadel, B. (2010). Arabidopsis and primary photosynthetic metabolism - more than the icing on the cake. Plant J. 61: 1067–1091.

Stockhaus, J., Schell, J., and Willmitzer, L. (1989). Correlation of the expression of the nuclear photosynthetic gene ST-LS1 with the presence of chloroplasts. EMBO J. 8: 2445–2451.

Szecowka, M., Heise, R., Tohge, T., Nunes-Nesi, A., Vosloh, D., Huege, J., Feil, R., Lunn, J., Nikoloski, Z., Stitt, M., Fernie, A.R., and Arrivault, S. (2013). Metabolic fluxes in an illuminated Arabidopsis rosette. Plant Cell 25: 694–714.

Thalmann, M., Pazmino, D., Seung, D., Horrer, D., Nigro, A., Meier, T., Kölling, K., Pfeifhofer, H.W., Zeeman, S.C., and Santelia, D. (2016). Regulation of leaf starch degradation by abscisic acid is important for osmotic stress tolerance in plants. Plant Cell 28: 1860–1878.

Timm, S., Florian, A., Arrivault, S., Stitt, M., Fernie, A.R., and Bauwe, H. (2012a). Glycine decarboxylase controls photosynthesis and plant growth. FEBS Lett. 586: 3692–3697.

Timm, S., Florian, A., Wittmiß, M., Jahnke, K., Hagemann, M., Fernie, A.R., and Bauwe, H. (2013). Serine acts as a metabolic signal for the transcriptional control of photorespiration-related genes in Arabidopsis. Plant Physiol. 162: 379–389.

Timm, S., Mielewczik, M., Florian, A., Frankenbach, S., Dreissen, A., Hocken, N., Fernie, A.R., Walter, A., and Bauwe, H. (2012b). High-to-low CO_2 acclimation reveals plasticity of the photorespiratory pathway and indicates regulatory links to cellular metabolism of Arabidopsis. PLoS One 7: e42809.

Timm, S., Wittmiß, M., Gamlien, S., Ewald, R., Florian, A., Frank, M., Wirtz, M., Hell, R., Fernie, A.R., and Bauwe, H. (2015). Mitochondrial dihydrolipoyl dehydrogenase activity shapes photosynthesis and photorespiration of Arabidopsis thaliana. Plant Cell 27: 1968–1984.

Usadel, B., Bläsing, O.E., Gibon, Y., Retzlaff, K., Höhne, M., Günther, M., and Stitt, M. (2008). Global transcript levels respond to small changes of the carbon status during progressive exhaustion of carbohydrates in Arabidopsis rosettes. Plant Physiol. 146: 1834–1861.

Weise, S.E., Schrader, S.M., Kleinbeck, K.R., and Sharkey, T.D. (2006). Carbon balance and circadian regulation of hydrolytic and phosphorolytic breakdown of transitory starch. Plant Physiol. 141: 879–886.

Wingler, A., Lea, P.J., Quick, W.P., and Leegood, R.C. (2000). Photorespiration: metabolic pathways and their role in stress protection. Philos. Trans. R. Soc. Lond. B Biol. Sci. 355: 1517–1529.

Winters, T.A., Henner, W.D., Russell, P.S., McCullough, A., and Jorgensen, T.J. (1994). Removal of 3′-phosphoglycolate from DNA strand-break damage in an oligonucleotide substrate by recombinant human apurinic/apyrimidinic endonuclease 1. Nucleic Acids Res. 22: 1866–1873.

Zanella, M., Borghi, G.L., Pirone, C., Thalmann, M., Pazmino, D., Costa, A., Santelia, D., Trost, P., and Sparla, F. (2016). β-Amylase 1 (BAM1) degrades transitory starch to sustain proline biosynthesis during drought stress. J. Exp. Bot. 67: 1819–1826.

Zelitch, I. (1975). Getting more CO_2 into food. Nature 256: 90–91.

Zhang, Q., Lee, J., Pandurangan, S., Clarke, M., Pajak, A., and Marsolais, F. (2013). Characterization of Arabidopsis serine:glyoxylate aminotransferase, AGT1, as an asparagine aminotransferase. Phytochemistry 85: 30–35.